Catal Lett (2008) 120:8–13
DOI 10.1007/s10562-007-9245-z

The State and Reactivity of Pt_6 Particles in ZSM-5 Zeolite

M. N. Mikhailov · L. M. Kustov · V. B. Kazansky

Received: 25 July 2007 / Accepted: 15 August 2007 / Published online: 7 September 2007

Abstract The density functional theory (DFT/B3LYP) calculations were applied to investigate the interaction of a Pt_6 particle with the ZSM-5 zeolite framework. The electronic structure of the metal particle is strongly affected by the interaction with basic framework oxygens and acid sites of the zeolite support. Adsorption on basic sites (E_{ads} = 6 kcal/mol) favors the formation of the electron enriched metal cluster. Interaction of the platinum cluster with the acid site characterized by stabilization energy of 47 kcal/mol results in oxidation of the metal particle and suppression of Brønsted acidity of the support. The hypothesis is put forward that the oxidized platinum particle can function as an active site for the alkane isomerisation on platinum supported high silica zeolites.

Keywords ZSM-5 zeolite · Pt_6 particle · Reverse spillover · Alkane isomerisation

1 Introduction

Fine metal particles supported on different oxides such as silica, alumina and zeolites are highly active in dehydrogenation, isomerization and hydrocracking of alkanes [1–9]. It is generally accepted that in a dual-function catalyst, hydrogenation and dehydrogenation occur on a metal particle, whereas isomerization proceeds on an acid site [10, 11]. This picture suggests two different kinds of sites and a negligible mutual influence among metal and acid sites [12]. However, this concept has been questioned in a number of recent works.

Freund and co-workers [13, 14] using infrared and photoelectron spectroscopies presented evidence that on introducing rhodium particles on the alumina surface the concentration of the surface hydroxyls decreases. At the same time, rhodium 3d-bands shift to higher binding energies. This observation indicates a strong interaction between metal particles and surface hydroxyls resulting in oxidation and stabilization of the supported metal particles.

Based on X-ray spectroscopic data, Sachtler and Stakheev showed that metal clusters supported on acid zeolites are electron deficient [15] and the extent of deficiency increases with acidity [16]. This observation can be interpreted as due to the electron transfer from the metal particle to the neighboring Brønsted acid site [17]. The electron deficiency of metal particles is also supported by the frequency shift in the infrared spectra of adsorbed CO [18–20].

Koningsberger et al. [21, 22] applied X-ray absorption spectroscopy to investigate the effect of the support on the electronic structure of supported metal particles. Hydrogen adsorption on platinum particles revealed that the increase in the support acidity shifts the Fermi level to higher binding energies and enhances the difference between Fermi level and platinum – hydrogen antibonding state [23, 24].

In a recent paper, Murzin and other authors [25] reported that the extent of the modification of the electronic structure of platinum particles supported on zeolites is dependent on the acid site strength. They indicated that the presence of platinum reduces the concentration of acid sites and in some cases completely suppresses both Brønsted and Lewis acidity.

In addition to experimental data, valuable information about the metal–oxide support interaction can be obtained

M. N. Mikhailov (✉) · L. M. Kustov · V. B. Kazansky
N.D. Zelinsky Institute of Organic Chemistry, Russian Academy of Sciences, Leninsky Prospect 47, Moscow 119991, Russian Federation
e-mail: mik@ioc.ac.ru

from quantum-chemical calculations. The interaction between metal particles and H form of X zeolite was studied by Rösch et al. [26, 27]. According to these results, the interaction between metal particles and Brønsted acid sites leads to the transfer of hydrogen atoms of hydroxyls onto the metal surface and to the oxidation of the metal particle.

In a more recent work [28] the interaction of platinum atom with HZSM-5 zeolite was investigated by means of the density functional theory. It was found that a platinum atom interacts with a Brønsted proton and the nearest framework oxygen. As the result, the electron density is transferred from oxygen to the metal atom. The proton of the Brønsted site stabilizes the platinum atom by withdrawing the excess of electron density.

All these results indicate that there is a strong interaction between metal particles and oxide support whereby the platinum particle oxidizes and the strength and concentration of the acid sites decrease. If this picture is correct, the question arises as to the nature of active sites in bifunctional platinum containing zeolites. It is therefore of interest to clarify the structural and catalytic implications of suppression of acidity in supported high-silica zeolites. In particular, the following aspects merit further consideration:

1. the energetics of the interaction of platinum particles with the high-silica zeolite framework;
2. the changes in the structures of a metal particle and zeolite in the course of interaction;
3. the change in the reactivity of supported platinum particles.

The present investigation was focused on the quantum chemical study (DFT/B3LYP) of the structure and reactivity of a Pt_6 cluster supported on ZSM-5 zeolite.

2 Computational Details

To model the fragment of ZSM-5 zeolite, the cluster approach was used. The cluster includes fourteen Si atoms and one Al atom and is based on the ten ring from the straight channel of zeolite. The cluster broken bonds (Si–O and Al–O) were saturated with hydrogens, placed at the 1.6 and 1.5 Å along Al–O and Si–O bonds, respectively. All terminal hydrogens were fixed during the geometry optimization. The positive charge of the lattice is compensated by the proton (H25) forming the Brønsted acid site (Fig. 1). The obtained cluster has the stoichiometry $HAlSi_{14}O_{18}H_{24}$. The cluster electronic structure was computed at the density functional theory (DFT) level using the Becke's three parameters exchange functional (B3) [29] combined with the Lee-Yang-Parr (LYP) [30] and Vosko-Wilk-Nusair (VWN5) [31] correlation functionals. The SBKJC effective core potential [32] and corresponding basis set augmented with polarization functions were used on all atoms. All the calculations were performed with the PC GAMESS [33, 34] program package. All the charges were calculated using natural populations [35].

3 Results and Discussion

The optimized clusters modeling the main intermediates of the interaction of the platinum particle with the ZSM-5 zeolite fragment are presented in Fig. 2a. The natural charges and electronic configurations of atoms in the clusters are presented in Table 1.

The adsorption interaction of the ZSM-5 zeolite and Pt_6 particle (electronic configuration $5d^{9.41}6s^{0.55}$, the Pt–Pt bond length is 2.69 Å) is characterized by very low adsorption energy (6 kcal/mol) and affords adsorption complex **1a**. However, as a result of adsorption, the geometric parameters of the metal particle change significantly: the Pt1–Pt5, Pt1–Pt6, Pt2–Pt4, Pt3–Pt6, and Pt2–Pt3 bonds shorten by 0.12–0.18 Å, and the Pt1–Pt4, Pt2–Pt5, Pt2–Pt6, Pt1–Pt3, Pt5–Pt6, and Pt3–Pt4 bonds elongate by 0.12–0.26 Å. The Pt4–Pt5 bond remains practically unchanged (shortens by 0.02 Å). The Al–O and Si–O bond lengths of the zeolite framework change by 0.01–0.02 Å. The cluster particle is localized in the ZSM-5 zeolite channel and interacts with the basic oxygen anions of the lattice (the Pt–O bond lengths are 2.3–2.6 Å). Due to this interaction, the electronic density on the s- and d-orbitals of the Pt2, Pt3, and Pt4 atoms increases (see Table 1). The Pt1, Pt5, and Pt6 atoms bear small positive charges. The Pt_6 cluster is polarized and has a negative total charge. Adsorption on basic sites of the support favors the formation of an electron enriched metal cluster. The reason for the appearance of the negative charge is a redistribution of the electron density from the Si and Al atoms through the O atoms of the zeolite framework onto the metal particle. The transfer of the Brønsted proton (H25) to the metal particle surface, the so-called reverse spillover, affords surface structure **2a**. In cluster **2a**, the Pt2–Pt6, Pt1–Pt4, and Pt1–Pt3 bonds elongate to 3.02–3.10 Å, and the Pt3–Pt4 distance increases to 3.19 Å. The adsorbed state of atomic hydrogen ($1s^{0.46} \rightarrow 1s^{0.99}$) is formed at the Pt1–Pt4 edge with the Pt1–H25 and Pt4–H25 bond lengths equal to 1.75 and 1.67 Å, respectively. The Pt1 ($5d^{9.28}6s^{0.63} \rightarrow 5d^{9.12}6s^{0.62}$) and Pt4 ($5d^{9.34}6s^{0.65} \rightarrow 5d^{9.16}6s^{0.56}$) atoms are oxidized gaining charges of 0.21 and 0.22, respectively. The decrease in the electron density is also observed on other Pt atoms. The total charge of the metal particle with the transferred Brønsted proton is 0.51. The reverse spillover process is of exothermic nature and

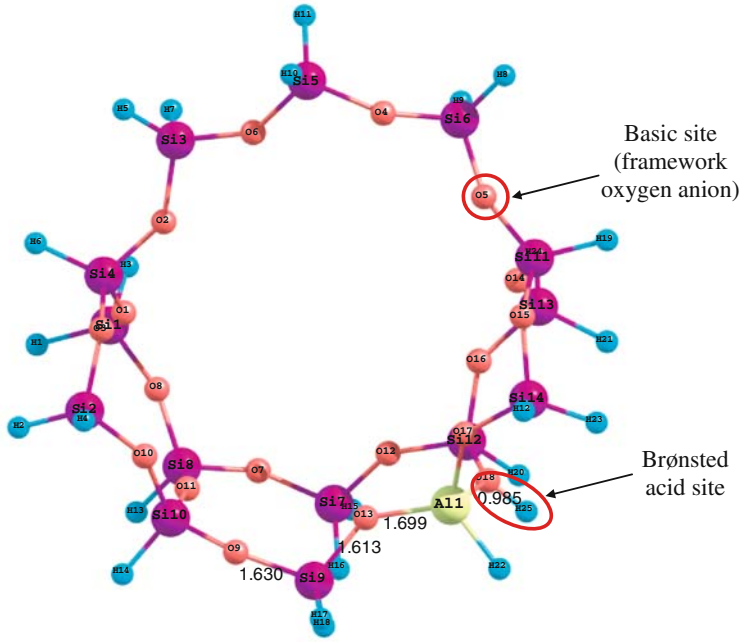

Fig. 1 Cluster modeling the ZSM-5 zeolite framework

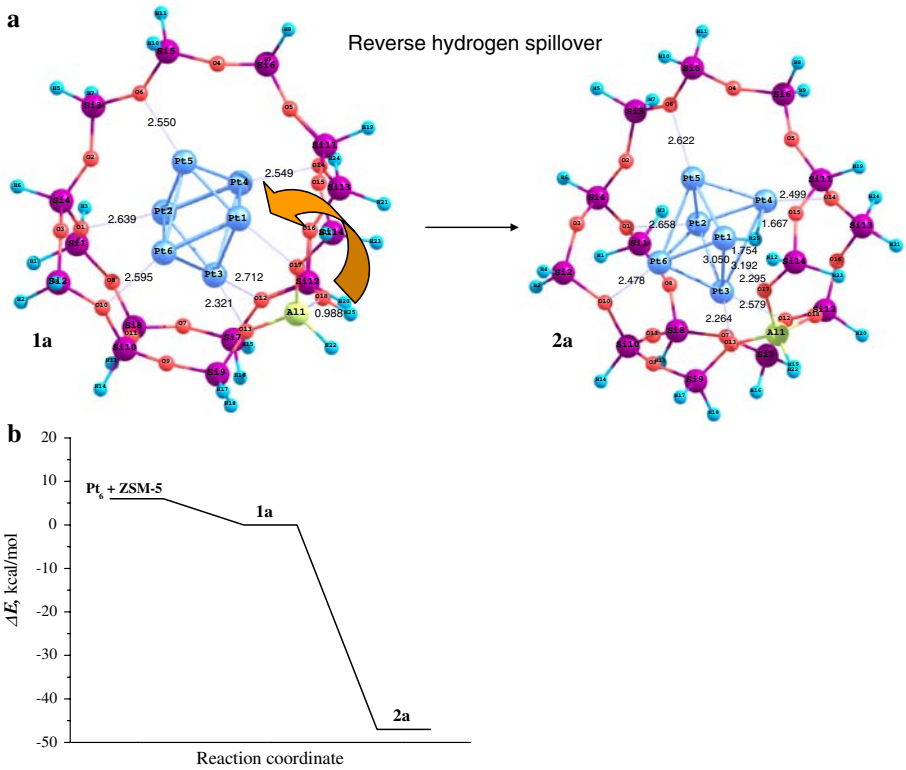

Fig. 2 (**a**) Optimized clusters modeling the intermediates of interaction of the Pt_6 particle with the zeolite framework. (**b**) Cross-section of the potential energy surface for interaction of the Pt_6 particle with the zeolite framework

proceeds with a zero activation energy. The acid site appears to stabilize the platinum particle and the stabilization energy can be estimated as close to 47 kcal/mol (Fig. 2b). Introduction of platinum into ZSM-5 zeolite results in a considerable reduction of the Brønsted acidity. Analysis of Table 2 shows that the immobilization of the Pt_6 cluster in the ZSM-5 zeolite channel induces the shift of the Fermi level toward lower binding energies by 1.64 eV and an increase in the band gap by 0.26 eV. The transfer of the Brønsted proton to the metal particle results in the shift of the Fermi level toward higher binding energies from –3.38 to –4.33 eV and increases the band gap up to 1.44 eV.

Table 1 Natural charges and electronic configurations of atoms in clusters 1a and 2a

	ZSM-5	1a	2a
O12	–1.29 ($2s^{1.74}2p^{5.55}$)	–1.30 ($2s^{1.73}2p^{5.55}$)	–1.31 ($2s^{1.75}2p^{5.55}$)
O13	–1.35 ($2s^{1.76}2p^{5.58}$)	–1.37 ($2s^{1.76}2p^{5.60}$)	–1.36 ($2s^{1.76}2p^{5.58}$)
O17	–1.35 ($2s^{1.76}2p^{5.58}$)	–1.36 ($2s^{1.76}2p^{5.59}$)	–1.34 ($2s^{1.77}2p^{5.55}$)
O18	–1.15 ($2s^{1.74}2p^{5.39}$)	–1.16 ($2s^{1.74}2p^{5.40}$)	–1.37 ($2s^{1.76}2p^{5.60}$)
Al1	1.87 ($3s^{0.45}3p^{0.66}$)	1.90 ($3s^{0.43}3p^{0.64}$)	1.90 ($3s^{0.44}3p^{0.63}$)
Si12	2.24 ($3s^{0.62}3p^{1.08}$)	2.26 ($3s^{0.61}3p^{1.07}$)	2.24 ($3s^{0.62}3p^{1.08}$)
H25	0.54 ($1s^{0.46}$)	0.54 ($1s^{0.46}$)	0.01 ($1s^{0.99}$)
Pt1	–	0.04 ($5d^{9.28}6s^{0.63}$)	0.21 ($5d^{9.12}6s^{0.62}$)
Pt2	–	–0.10 ($5d^{9.42}6s^{0.63}$)	–0.08 ($5d^{9.35}6s^{0.69}$)
Pt3	–	–0.05 ($5d^{9.34}6s^{0.65}$)	0.22 ($5d^{9.16}6s^{0.56}$)
Pt4	–	–0.15 ($5d^{9.46}6s^{0.63}$)	0.03 ($5d^{9.32}6s^{0.60}$)
Pt5	–	0.03 ($5d^{9.34}6s^{0.58}$)	0.10 ($5d^{9.30}6s^{0.56}$)
Pt6	–	0.02 ($5d^{9.38}6s^{0.55}$)	0.05 ($5d^{9.28}6s^{0.62}$)
Pt_6	–	**–0.21**	**0.51**

Table 2 Calculated natural charges (q), energy of Fermi level (E_f), band gap (E_{bg}) and frequency of adsorbed CO for the Pt_6 particle and clusters 1a,2a

Cluster	q(Pt_6)	E_f, eV	E_{bg}, eV	ν(CO), cm^{-1}	$\Delta\nu$(CO), cm^{-1}
Pt_6	0.00	–5.02	1.42	2051	0
1a	–0.21	–3.38	1.16	2042	–9
2a	0.51	–4.33	1.44	2063	12

When compared to the isolated Pt_6 particle, the cluster **2a** is characterized by the Fermi level shifted toward a lower binding energy by 0.69 eV with nearly the same band gaps.

When loaded in the zeolite, platinum particles tend to be oxidized. Some support for this suggestion is provided by the calculated frequencies of carbon monoxide adsorbed on the metal particle (Table 2). Comparison of the CO frequency shift observed on a supported metal particle with that on an isolated metal cluster gives evidence for the magnitude and sign of the charge on the metal particle. In the case of a positive shift, the particle is positively charged. In the reverse case, the charge of a particle seems to be negative.

Our data indicate that the platinum cluster accommodated in the zeolite channel has a negative charge and the frequency of adsorbed CO shows a negative shift. The proton transfer leads to the formation of cationic platinum species as evidenced by a positive CO frequency shift of 12 cm^{-1}.

Introduction of platinum into zeolite results in a substantial decrease in the number of Brønsted acid sites or even in their complete suppression. In addition, interaction of the platinum particle with acid sites generates the electron-deficient metal particles. These data serve to clarify the mechanism of alkane isomerisation on platinum supported zeolites. It is well known that solid acids loaded with platinum are used in the industrial isomerisation process. The catalysts are often called bifunctional. One function is a function of an acid catalyst, the other being a function of a hydrogenation–dehydrogenation catalyst. Thus, it is supposed that alkane is first dehydrogenated on metal sites to the corresponding alkene, which is then isomerised on acid sites into a branched alkene. The branched alkene is subsequently hydrogenated into the branched alkane again on the metal site. However, from the

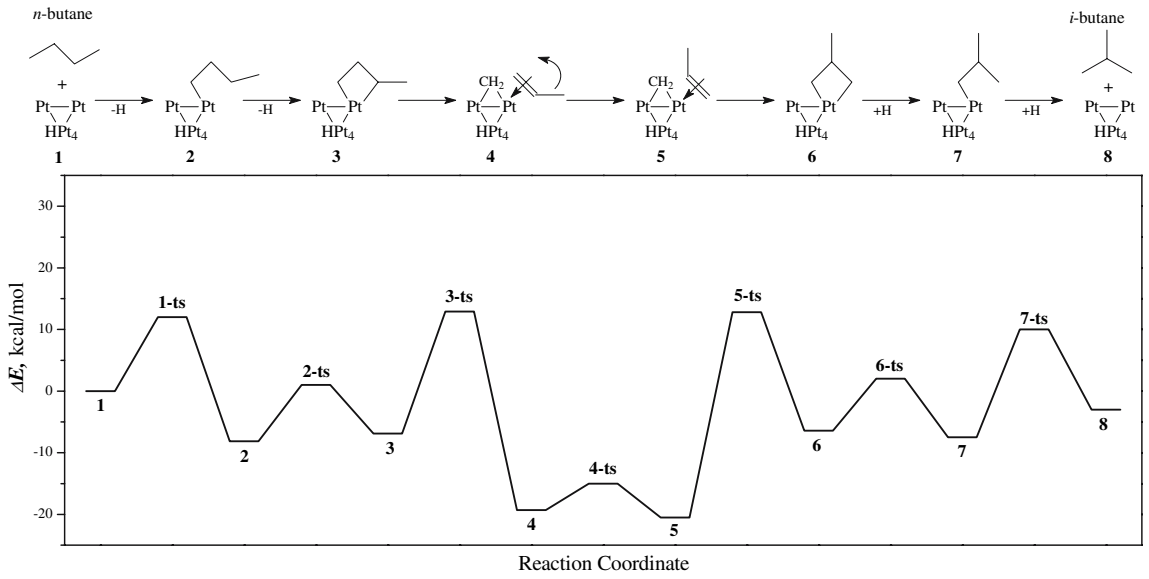

Fig. 3 Scheme and energy profile for butane isomerisation on a Pt_6H^+ particle

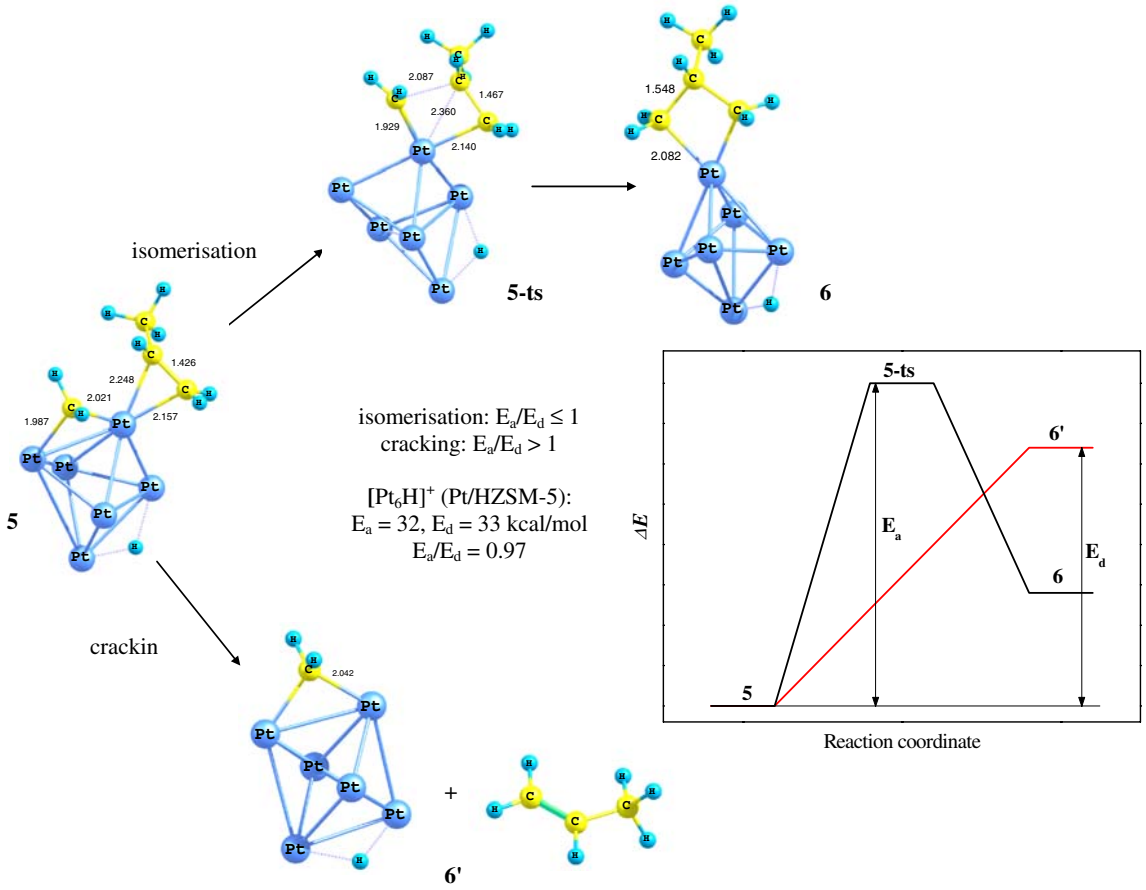

Fig. 4 Butane isomerisation vs. cracking on a Pt_6H^+ particle

results outlined above, it follows that in the presence of platinum the number of acid sites decreases. Also, as it was shown [36], the Brønsted acid site weakening takes place due to the interaction with metal particles as a result of the charge transfer between the proton and the metal. Accordingly, the bifunctional mechanism might not be always operative in the alkane isomerisation on platinum supported zeolites.

It can be proposed that the role of the acid site can be the oxidation of the platinum particle and the oxidized species can be an active site in alkane isomerisation. A simple model of the active site represented by a positively charged Pt_6H^+ cluster can be used to illustrate this hypothesis. As a model reaction, the *n*-butane isomerisation can be considered.

Figure 3 shows a scheme describing the proposed mechanism of butane isomerisation on a charged platinum cluster. In contrast to the conventional bifunctional mechanism, this mechanism involves a metal-cyclobutane intermediate as was earlier suggested to describe the alkane isomerisation over molybdenium oxycarbide [37]. Alkane transformation occurs on a single active site represented by a charged metal particle. At the first step, butane oxidative addition to the platinum atom results in the butyl surface structure **2** and proceeds with an activation energy of 12 kcal/mol. Then hydrogen transfer from the butyl fragment of the cluster **2** to the same platinum atom leads to the metal-cyclobutane complex **3**. At the next step, the C–C bond in the metal-cyclobutane derivative is broken to form the surface carbene species coordinatively bound to two platinum atoms and π-bonded propene, structure **4**. The **3** → **4** step is of exothermic nature (ca. 10 kcal/mol) and is characterized by an activation energy of 20 kcal/mol. Then π-bonded propene rotates and recombines with surface carbene to yield metal-isocyclobutane complex **6**. The barrier to propene rotation does not exceed 5 kcal/mol, and the activation energy of recombination of surface carbene and π-bonded propene is below 35 kcal/mol. Finally, the hydrogenation of structure **6** gives isobutane and regenerates the initial platinum cluster.

While analyzing the potential energy surface for butane isomerisation on a positively charged platinum cluster, three important features can be readily observed:

1. The energy surface includes a very stable surface carbene entity as the main intermediate;
2. The barriers for hydrogenation and dehydrogenation slightly increase but still remain below 20 kcal/mol;
3. The activation energies for C–C bond cleavage and formation does not exceed 35 kcal/mol.

Now it is of interest to consider in detail the key step of isomerisation, recombination of surface carbene with propene. One can discriminate two different ways of transformation of surface carbene with π-bonded propene (Fig. 4). The first one is the isomerisation to form metal-isocyclobutane structure 6 involving transition state **5-ts** and the second one is the cracking accompanied by propene desorption (**6′**). A preferred way of the transformation strongly depends on the E_a/E_d ratio. E_a is the activation energy of carbene to metal-cyclobutane transformation and E_d is the desorption energy of propene as shown in the inset of Fig. 4. If this ratio is above unity, the cracking path prevails; in other cases, the isomerisation is preferred. For the charged particle, this ratio is close to unity and the isomerisation is the main direction.

4 Conclusions

The results obtained in the present work clearly show that the interaction between a platinum particle and the high-silica zeolite framework is mutual. It appears that the interaction of the platinum particle with basic framework oxygens and acid sites of the zeolite support has a significant impact on the electronic structure of the metal. The introduction of the platinum cluster in the zeolite channel results in the reverse hydrogen spillover from the Brønsted acid site onto the metal surface. This in turn leads to oxidation of the metal particle and suppression of Brønsted acidity of the zeolite support. Adsorption on basic sites of the support favors the formation of electron-enriched metal clusters. It is possible that the oxidized platinum particles can act as active sites for the alkane isomerisation on platinum supported catalysts. It can be further speculated that a conventional route typical to bifunctional catalysts can be supplemented by the proposed alternative mechanism involving oxidized metal species.

References

1. Bandiera J, Naccache C, Imelik B (1978) J Chim Phys–Chim Biol 75:406
2. Chupin J, Gnep NS, Lacombe S, Guisnet M (2001) Appl Catal A 206:43
3. Blomsma E, Martens JA, Jacobs PA (1997) Stud Surf Sci Catal B 105:909
4. Galperin LB, Bricker JC, Holmgren JR (2003) Appl Catal, A 239:297
5. Sugioka M, Tochiyama C, Matsumoto Y, Sado F (1995) Stud Surf Sci Catal 94:544
6. Vasina TV, Masloboishchikova OV, Khelkovskaya-Sergeeva EG, Kustov LM, Houzvička JI (2001) Stud Surf Sci Catal 138:93
7. Arribas MA, Martinez A (2002) Appl Catal A 230:203
8. Noordhoek NJ, Schuring D, de Gauw FJMM, Anderson BG, de Jong AM, de Voigt MJA, van Santen RA (2002) Ind Eng Chem Res 41:1973
9. Kuznetsov PN (2003) J Catal 218:2
10. Weisz PB, Swegler EW (1957) Science 126:31
11. Kuhlmann A, Roessner F, Schwieger W, Gravenhorst O, Selvam T (2004) Catal Today 97:303
12. Ono Y (2003) Catal Today 81:3
13. Libuda J, Frank M, Sandell A, Andersson S, Brühwiler PA, Bäumer M, Mårtensson N, Freund H-J (1997) Surf Sci 384:106
14. Heemeier M, Frank M, Libuda J, Wolter K, Kuhlenbeck H, Bäumer M, Freund H-J (2000) Catal Lett 68:19
15. Stakheev AYu, Sachtler WMH (1991) J Chem Soc, Faraday Trans 87:3703
16. Blackmond DG, Goodwin JG Jr (1981) J Chem Soc Chem Commun 125
17. Sachtler WMH, Zhang Z (1993) Adv Catal 39:129
18. Vaarkamp M, Miller JT, Modica FS et al. (1993) Stud Surf Sci Catal 75:809
19. Zholobenko VL, Lei GD, Carvill BT et al. (1994) J Chem Soc, Faraday Trans 90:233
20. Weber RS, Boudart M, Gallezot P (1980) Stud Surf Sci Catal 4:415
21. Ramaker DE, Mojet BL, Garriga Oostenbrink MT, Miller JT, Koningsberger DC (1999) Phys Chem Chem Phys 1:2293
22. Hammer B, Nørskov JK (1995) Nature 376:238
23. Koningsberger DC, Oudenhuijzen MK, Bitter JH, Ramaker DE (2000) Topics Catal 10:167
24. Koningsberger DC, Ramaker DE, Miller JT, de Graaf J, Mojet BL (2001) Topics Catal 15:35
25. Kubička D, Kumar N, Venäläinen T, Karhu H, Kubičková I, Österholm H, Murzin YuD (2006) J Phys Chem, B 110:4937
26. Vayssilov GN, Gates BC, Rösch N (2003) Angew Chem Int Ed 42:1391
27. Vayssilov GN, Rösch N (2005) Phys Chem Chem Phys 7:4019
28. Treesukol P, Srisuk K, Limtrakul J, Truong TN (2005) J Phys Chem, B 109:11940
29. Becke AD (1993) J Chem Phys 98:5648
30. Lee C, Yang W, Parr RG (1988) Phys Rev B 37:785
31. Vosko SH, Wilk L, Nusair M (1980) Can J Phys 58:1200
32. Stevens WJ, Krauss M, Basch H, Jasien PG (1992) Can J Chem 70:612
33. Granovsky AA, PC GAMESS version 7.0, http://classic.chem.msu.su/gran/gamess/index.html
34. Schmidt MW, Baldridge KK, Boatz JA et al. (1993) J Comput Chem 14:1347
35. NBO 4.M. Glendening ED, Badenhoop JK, Reed AE, Carpenter JE, Weinhold F (1999) Theoretical Chemistry Institute, University of Wisconsin, Madison, WI
36. Stakheev AY, Kustov LM (1999) Appl Catal, A 188:3
37. Blekkan E, Pham-Huu C, Ledoux MJ, Guille J (1994) Ind Eng Chem Res 33:1657